Zagazig University Medical Journal
www.zumj.journals.ekb.eg
https://doi.org/10.21608/zumj.2025.392468.3991 Volume 31, Issue 9 September. 2025
Manuscript ID:ZUMJ-2506-3991
DOI:10.21608/zumj.2025.392468.3991

ORIGINAL ARTICLE

Structure-Based Identification of Selective Phytochemical Inhibitors Targeting EmCoASY: A Novel Therapeutic Strategy Against Alveolar Echinococcosis

Abdulbaset Mohammad M Kabli [1*]

[1]Laboratory Medicine Department, Faculty of Applied Medical Sciences, Al-Baha University, Al-Baha, Kingdom of Saudi Arabia

***Corresponding author:**
Abdulbaset Mohammad M Kabli

E-mail:
akabli@bu.edu.sa

Submit Date 10-06-2025
Revise Date 18-07-2025
Accept Date 11-08-2025

ABSTRACT

Background: Alveolar echinococcosis (AE), caused by the larval stage of *Echinococcus multilocularis*, is a life-threatening zoonotic disease with limited treatment options due to chemotherapy-associated toxicity and incomplete parasitic clearance. The aim of this study was to identify selective phytochemical inhibitors targeting dephospho-CoA synthase (EmCoASY), a critical enzyme for parasite survival, using a structure-based drug discovery approach.

Methods: A total of 419 phytochemicals with reported antiparasitic or antimalarial activity were collected from literature and databases. After structure retrieval from PubChem, 297 compounds were subjected to ADMET screening using SwissADME and pkCSM tools. Toxicity-based filtering shortlisted 20 compounds. These were docked against EmCoASY and its human homolog (HsCoASY) to assess binding affinity and selectivity. Top candidates underwent 200 ns molecular dynamics (MD) simulations, including RMSD, RMSF, principal component, covariance matrix, and hydrophobic surface analyses. MM/GBSA calculations were performed to estimate binding free energies.

Results: Chaparrinone (CID: 73154) and artesunate (CID: 6917864) showed strong binding affinities (-8.9 and -8.2 kcal/mol) to EmCoASY with minimal interaction with HsCoASY. Molecular dynamics simulations revealed stable protein-ligand complexes with reduced conformational fluctuations. MM/GBSA analysis indicated that chaparrinone had the most favorable binding energy, driven by and lipophilic interactions.

Conclusions: This structure-based in silico study identifies chaparrinone and artesunate as promising selective inhibitors of EmCoASY. Their favorable selectivity, stability, and binding energetics support their potential as novel therapeutic agents for alveolar echinococcosis. Further in vitro and in vivo validation studies are recommended to confirm their efficacy and safety.

Keywords: Alveolar echinococcosis; *Echinococcus multilocularis*; Dephospho-CoA synthase; Molecular docking; Phytochemical.

INTRODUCTION

Alveolar echinococcosis (AE) is a life-threatening zoonotic disease caused by the larval stage of the tapeworm *Echinococcus multilocularis*. This disease, characterized by infiltrative, tumor-like lesions primarily in the liver, resembles malignant tumors in growth and progression and is associated with high mortality if left untreated[1]. AE is endemic to the Northern Hemisphere, with increasing incidence reported in Europe, Asia, and North America. Current therapeutic options, including benzimidazole-based chemotherapy and surgical resection, are limited and often ineffective.

Benzimidazoles, though effective at parasitostasis, require prolonged treatment and exhibit considerable toxicity, while surgical interventions are often precluded due to lesion invasiveness and the risk of recurrence. These limitations highlight the urgent need for novel, selective therapeutic strategies for AE[2–5].

Targeting metabolic pathways essential for parasite survival, but absent or highly divergent from those of the host, has emerged as a promising approach in antiparasitic drug discovery. One such target is Dephospho-CoA kinase (EmCOASY), an enzyme catalyzing the phosphorylation of dephosphopantetheine to coenzyme A (CoA), a molecule vital for energy metabolism, fatty acid synthesis, and numerous biosynthetic pathways[6,7]. Recent studies have demonstrated that the CoA biosynthesis pathway is critical for *E. multilocularis* survival and proliferation, particularly due to its essential role in maintaining parasite energy metabolism and membrane biosynthesis. Notably, EmCOASY exhibits significant structural and functional divergence from its human homolog (HsCOASY), particularly in the architecture of the binding pocket and key catalytic residues, suggesting the feasibility of selective inhibition with minimal off-target effects in humans[8,9].

Structural analyses, including high-confidence predictions via AlphaFold2, have revealed unique domain arrangements in EmCOASY, such as the presence of P-loop NTPase, cytidyltransferase-like, and Rossmann-fold domains, which coordinate substrate binding and catalysis. Transcriptomic analyses have shown that EmCOASY is highly expressed in the germinal layer of the parasite, the site of active proliferation and metabolic activity, indicating its essentiality for parasite viability. Recent computational and experimental research in related parasites, including *Plasmodium falciparum* and *Leishmania* species, has demonstrated the efficacy of targeting CoA biosynthesis enzymes, further underscoring the potential of EmCOASY as a drug target in *E. multilocularis*[10,11].

To explore selective inhibition of EmCOASY, an integrated in silico approach combining structural prediction, pocket identification, molecular docking, and dynamic simulation was employed. The predicted structure of EmCOASY was validated using MolProbity, and potential binding pockets were identified with CASTpFold. A curated library of antiparasitic compounds, selected through a comprehensive literature review and validated for pharmacokinetic properties and toxicity via SwissADME and pkCSM, was subjected to molecular docking using AutoDock Vina within the PyRx virtual screening platform. Comparative docking against HsCOASY provided an assessment of ligand selectivity and potential off-target effects. Molecular dynamics simulations, performed using GROMACS, captured the stability and conformational dynamics of protein-ligand complexes, with binding free energy calculations conducted through MM-GBSA analysis to quantify interaction strengths.

To ensure robustness and specificity of the docking results, decoy-based validation was performed by generating structurally similar but biologically inactive compounds for each high-affinity ligand. These decoys were subjected to identical docking conditions, and comparative analyses of binding affinities and interaction profiles were used to confirm the selectivity and predictive power of the docking approach[12,13].

Saliba and Spry (2021) reviewed the CoA biosynthesis pathways in Apicomplexan parasites, including *Plasmodium* species, emphasizing the suitability of these pathways as drug targets. The study

highlighted the structural and mechanistic differences between parasite and human CoA biosynthetic enzymes, suggesting opportunities for selective inhibition[14]. Another study demonstrated the dual inhibition of the electron transport chain (ETC) and malate dismutation (MD) pathways in *E. multilocularis*. The study found that simultaneous targeting of these energy-generating pathways using specific inhibitors significantly impaired parasite viability, proposing a novel therapeutic approach for alveolar echinococcosis[15]. These studies collectively reinforce the strategy of targeting unique metabolic and regulatory pathways in parasitic organisms, such as CoA biosynthesis and specific kinases, to develop selective and effective treatments for diseases like alveolar echinococcosis[16].

This comprehensive,-computational strategy leverages cutting-edge bioinformatics and cheminformatics techniques to identify potent, selective inhibitors of, laying the groundwork for the development of novel therapeutics against alveolar echinococcosis.

METHODS

Target Selection and Sequence Extraction

Alveolar echinococcosis (AE), caused by *Echinococcus multilocularis*, represents a severe zoonotic threat with limited therapeutic options and increasing prevalence. Current treatments rely on benzimidazoles and surgery, both of which face challenges such as toxicity, poor bioavailability, and high recurrence rates. To address these challenges, *E. multilocularis* was selected as the target organism for in silico drug discovery due to its clinical significance and the availability of comprehensive genomic resources. Genome data for *Echinococcus multilocularis* were retrieved from WormBase ParaSite (https://parasite.wormbase.org) to enable systematic exploration of kinase-related proteins essential for parasite metabolism[17–19]. The GFF3 annotation file, genome assembly FASTA, and protein FASTA were downloaded from the same resource. Gene selection was based on functional annotations highlighting essential catalytic domains, including P-loop NTPase, cytidyltransferase-like, and Rossmann-fold motifs. The target gene identified encodes a bifunctional coenzyme A synthase containing a dephospho-CoA kinase domain (InterPro IPR001977), essential for coenzyme A biosynthesis and energy metabolism. This enzyme was prioritized for its conserved structure, absence of close human homologs, and predicted druggability.

Protein Structure Modeling

The amino acid sequence corresponding to the selected gene was extracted from the *Echinococcus multilocularis* protein FASTA file obtained from WormBase ParaSite. This sequence was then used as input for structural modeling using AlphaFold2, executed via Google Colab (https://colab.research.google.com) to predict the three-dimensional conformation of the target protein. AlphaFold2's deep learning-based approach enabled high-confidence modeling of the protein structure[20,21]. The resulting PDB file, representing the predicted three-dimensional structure, was retrieved for downstream analyses, including binding site prediction, molecular docking, and dynamics simulations[22]. To evaluate the selectivity of potential inhibitors targeting the *Echinococcus multilocularis* dephospho-CoA kinase, the human homolog, Coenzyme A synthase (COASY), was selected as a negative control. COASY is a bifunctional enzyme catalyzing the final two steps in coenzyme A biosynthesis, including the dephospho-CoA kinase activity. The amino acid sequence of human COASY was retrieved from the UniProt database (UniProt ID: Q13057). Due to the absence

of a full-length experimentally determined structure in the Protein Data Bank (PDB), a high confidence predicted 3D structure was obtained from the AlphaFold Protein Structure Database (https://alphafold.ebi.ac.uk/entry/Q13057). This model was utilized for comparative structural analyses and molecular docking studies to assess the specificity of candidate compounds and minimize potential off-target interactions with the human enzyme.

Sequence Alignment

Protein sequences of *Echinococcus multilocularis* Dephospho-CoA kinase (EmCOASY) and human Coenzyme A synthase (HsCOASY) were retrieved from WormBase ParaSite and UniProt (UniProt ID: Q13057), respectively. Multiple sequence alignment (MSA) was performed using the online Clustal Omega tool available through EMBL-EBI (https://www.ebi.ac.uk/Tools/msa/clustalo/)[23,24]. The resulting alignment was visualized and analyzed using Jalview software (https://www.jalview.org) and MView (https://desmid.github.io/mview/) to highlight conserved and divergent regions. The alignment visualization was exported as a PNG file for inclusion in the manuscript.

Structural Validation and Geometric Assessment

The predicted three-dimensional structural models of *Echinococcus multilocularis* Dephospho-CoA kinase (EmCOASY) and human Coenzyme A synthase (HsCOASY) obtained from AlphaFold2 were validated using the MolProbity web server (http://molprobity.biochem.duke.edu/). MolProbity evaluates structural quality by analyzing key geometric parameters, including backbone dihedral angles, sidechain rotamer conformations, steric clashes, and Ramachandran plot distributions[25,26]. The Protein Data Bank (PDB) format files for both parasite and human protein models were uploaded to MolProbity independently, and the resulting structural validation metrics were retrieved. These assessments confirmed the geometric reliability of both protein models, ensuring their suitability for accurate downstream molecular docking and comparative analyses.

Pocket analysis of the Proteins

The AlphaFold-predicted structural models of *Echinococcus multilocularis* Dephospho-CoA kinase (EmCOASY) and human Coenzyme A synthase (HsCOASY) were analyzed to identify and characterize potential ligand-binding pockets using the CASTpFold web server (https://cfold.bme.uic.edu/castpfold). CASTpFold applies alpha shape theory and Delaunay triangulation methodologies to predict and characterize binding sites on protein surfaces, providing detailed geometric parameters such as volume, surface area, and identification of lining residues[27]. The predicted structural models, saved in PDB format, were uploaded to the CASTpFold server, and default parameters were applied for pocket detection and mapping. Results included comprehensive descriptions of solvent-accessible surface areas (SASA), molecular surface areas (MSA), and volumes of the identified pockets, as well as detailed residue lists defining the boundaries of each pocket. This detailed pocket characterization enabled the selection of the most prominent and druggable binding sites, subsequently guiding accurate molecular docking and ligand-protein interaction analyses.

Ligand Selection for Therapeutic analysis

Ligand selection for this study was performed through an extensive literature review focusing exclusively on compounds with documented antiparasitic activities. Scientific databases, including PubMed, ScienceDirect, and Google Scholar, were systematically searched to identify compounds with validated efficacy against

various parasitic diseases. Additionally, Dr. Duke's Phytochemical and Ethnobotanical Database was consulted to uncover natural compounds exhibiting antiparasitic potential. Following initial identification, shortlisted compounds were queried in the PubChem database (https://pubchem.ncbi.nlm.nih.gov) to retrieve unique Compound Identifiers (CIDs) and their corresponding Simplified Molecular Input Line Entry System (SMILES) representations. These chemical descriptors were essential for accurate compound identification and subsequent in silico computational procedures, including molecular docking and pharmacokinetic profiling. This meticulous ligand selection and verification ensured that only well-characterized antiparasitic agents, relevant for potential inhibition of *Echinococcus multilocularis* Dephospho-CoA kinase (EmCOASY), were incorporated into the computational pipeline.

ADMET predictions of Selected ligands

The shortlisted ligands were evaluated through comprehensive ADMET (Absorption, Distribution, Metabolism, Excretion, and Toxicity) predictions to assess pharmacokinetic suitability and potential toxicological risks. ADMET analysis was conducted using SwissADME for absorption and physicochemical properties, and pkCSM for toxicity assessments[28]. Key parameters analyzed included blood-brain barrier (BBB) permeability, gastrointestinal (GI) absorption, Lipinski's rule-of-five violations, mutagenicity (AMES test), hepatotoxicity, and skin sensitization potential[29–32]. These predictions ensured the selected ligands exhibited favorable pharmacokinetic and safety profiles suitable for further drug development against *Echinococcus multilocularis*.

Molecular Docking Studies

Molecular docking simulations were conducted to evaluate binding affinities and interaction modes of selected ligands (identified from previous ADMET screening) against *Echinococcus multilocularis* Dephospho-CoA kinase (EmCOASY) and human Coenzyme A synthase (HmCOASY). Docking analyses served to assess ligand binding selectivity between the parasite and human homolog. Docking studies were executed using AutoDock Vina, implemented through the PyRx virtual screening platform[33]. Both receptor structures, EmCOASY and HmCOASY, were prepared as receptor files in PDBQT format (emcoasy.pdbqt and hmcoasy.pdbqt, respectively). Ligands underwent energy minimization and format conversion into PDBQT using Open Babel, ensuring accurate molecular geometry.

Docking parameters for EmCOASY were defined by setting the grid box based on CASTpFold pocket prediction results. The grid box was centered at coordinates (x = -0.9374, y = -0.0086, z = -1.3049) with dimensions (x = 89.30 Å, y = 70.26 Å, z = 65.78 Å) to encompass the entire binding site comprehensively. Similarly, docking against the human enzyme (HmCOASY) used a grid box centered at coordinates (x = 1.4246, y = 1.7532, z = -2.5058) with dimensions (x = 75.13 Å, y = 64.46 Å, z = 94.41 Å) to ensure complete coverage of the targeted binding site. An exhaustiveness parameter of 8 was utilized to thoroughly sample the ligand's possible binding conformations and orientations. Docking outcomes were ranked according to the lowest predicted binding energy values (ΔG) provided by AutoDock Vina. The highest-affinity binding poses were selected for subsequent detailed visualization and ligand-protein interaction analysis using PyMOL and Discovery Studio Visualizer. Critical interactions, including hydrogen bonds,

hydrophobic interactions, and π–π stacking, were systematically analyzed to confirm ligand compatibility and selectivity towards the binding pockets.

Decoy-Based Validation of High-Affinity Ligands

To assess the robustness and specificity of the docking results against *Echinococcus multilocularis* Dephospho-CoA kinase (EmCOASY), a decoy-based validation approach was conducted. For each ligand showing high binding affinity in molecular docking simulations, a set of 50 structurally similar but presumed inactive decoy molecules were retrieved from the Directory of Useful Decoys Enhanced (DUDE) database (https://dude.docking.org/)[34]. These decoy molecules were carefully selected based on structural similarity and comparable physicochemical properties to their corresponding active ligands, but with the expectation of no biological activity against EmCOASY. SMILES notations of the decoys were obtained from the DUDE database and converted into energy-minimized three-dimensional structures using the Open Babel software to ensure appropriate geometries for docking simulations. Each decoy molecule underwent molecular docking procedures identical to those used for the active ligands, including identical grid box settings and exhaustiveness parameters. Comparative analyses between the docking scores and interaction profiles of the active ligands and their corresponding decoys allowed for robust evaluation of ligand specificity and provided a critical negative control to strengthen confidence in the predictive accuracy of the docking methodology used for EmCOASY inhibitor identification.

Molecular Dynamics Simulation Studies

Molecular dynamics (MD) simulations were conducted to evaluate the stability, conformational flexibility, and protein-ligand interaction dynamics of the selected complexes. Simulations were performed using the GROMACS 2024 package with the CHARMM36-jul2022 force field applied to the proteins[35,36]. Ligand topology and parameters were accurately determined using the CHARMM General Force Field (CGenFF) through the online platform (https://cgenff.com)[37], ensuring reliable representation of ligand chemistry and interactions. Each protein-ligand complex was solvated in a cubic box filled with TIP3P water molecules, and sodium and chloride ions were introduced to neutralize the charge and maintain physiological ionic conditions.

Systems underwent initial energy minimization using the steepest descent algorithm to remove steric clashes and reach a low-energy state. Equilibration was performed in two stages: first, a 1 ns NVT ensemble (constant number, volume, temperature) equilibration was carried out at 300 K employing the V-rescale thermostat to achieve temperature stability. This was followed by a 1 ns NPT ensemble (constant number, pressure, temperature) equilibration maintained at 1 bar pressure using the Parrinello-Rahman barostat to stabilize pressure conditions. After equilibration, 200 ns production MD simulations were executed under periodic boundary conditions to capture comprehensive dynamic behavior.

Trajectory analyses were conducted using built-in GROMACS utilities. Structural stability and residue-level dynamics were quantified by calculating root mean square deviation (RMSD) and root mean square fluctuation (RMSF). Solvent-accessible surface area (SASA) and radius of gyration (Rg) analyses provided insights into protein compactness and surface exposure. Principal component analysis (PCA) and dynamic cross-correlation matrices (DCCM) were utilized to examine collective and correlated

motions within protein-ligand complexes. Binding free energies of complexes were estimated using the Molecular Mechanics Generalized Born Surface Area (MM-GBSA) approach implemented in the gmx_MMPBSA tool, assessing contributions from van der Waals interactions, electrostatics, and solvation (polar and non-polar) terms to gauge binding affinity and interaction stability.

RESULTS

Target Selection and Sequence Extraction

The genome assembly of *E. multilocularis* (assembly EMULTI002, BioProject PRJEB122, strain Java) was retrieved from the WormBase ParaSite database. This species is the causative agent of alveolar echinococcosis and is a priority for drug target exploration due to its lethal impact and emerging prevalence.

To identify potential drug targets, genome annotations were carefully examined for kinase-related proteins involved in essential biosynthetic pathways. A gene annotated as EmuJ_000009100, encoding a bifunctional coenzyme A synthase with a Dephospho-CoA kinase domain (IPR001977), was selected. Functional annotations revealed the presence of conserved cytidyltransferase-like (IPR004821), Rossmann-like fold (IPR014729), and P-loop NTPase (IPR027417) domains, crucial for ATP/CoA binding and catalytic activity. This enzyme plays a key role in Coenzyme A biosynthesis, an essential metabolic pathway in the parasite, with limited homology to human kinases, making it an attractive drug target **(Table S1).**

Using the GFF3 annotation file, the genomic coordinates of EmuJ_000009100 were identified on scaffold pathogen_EmW_scaffold_01 (positions 16,667,370 to 16,670,916, forward strand) (**Table S1).** The corresponding protein sequence (EmuJ_000009100.1) was extracted from the WormBase ParaSite protein FASTA file. This sequence comprises multiple conserved motifs and is suitable for downstream structural modeling, binding site prediction, and virtual screening.

Sequence Alignment Analysis

Sequence alignment between *Echinococcus multilocularis* Dephospho-CoA kinase (EmCOASY) and the human Coenzyme A synthase (HsCOASY) showed significant sequence divergence (overall identity: approximately 25.1%) despite high alignment coverage (94.3%). Conserved regions were mostly restricted to catalytic and functional domains, indicating structural conservation crucial for kinase activity. Importantly, several divergent residues were identified around the predicted substrate-binding sites, suggesting these regions as promising targets for selective inhibitor design. The clear sequence divergence between EmCOASY and the human homolog supports the hypothesis that selective therapeutic targeting of the parasite kinase is achievable without significant off-target effects in humans **(Figure S1).**

Structural Validation and Geometric Assessment

The structural integrity and stereochemical quality of the predicted protein models for *Echinococcus multilocularis* Dephospho-CoA kinase (EmCOASY) and its human homolog (HsCOASY) were rigorously evaluated using the MolProbity structure validation platform. The results revealed overall high-quality geometry for both models, with the majority of validation parameters falling within acceptable or near-optimal ranges, supporting their reliability for downstream docking and simulation analyses.

For EmCOASY, a total of 95.63% of residues were positioned within the favored regions of the Ramachandran plot, with an additional 3.79% in allowed regions and

only 0.57% classified as outliers. In the case of HsCOASY, 95.55% of residues were within favored regions, 3.74% in allowed regions, and 0.71% were outliers. Although both models slightly fell short of the ideal >98% favored threshold, the Ramachandran Z-scores (−1.32 for EmCOASY and −0.54 for HsCOASY) were well within acceptable limits ($|Z| < 2$), indicating no significant overall bias in backbone conformations **(Figure S2).**

Both models exhibited strong side-chain geometry, with 98.29% and 98.35% of rotamers in favored conformations for EmCOASY and HsCOASY, respectively. Poor rotamers were minimal, reported at 0.43% (EmCOASY) and 0.62% (HsCOASY), which were only marginally above the ideal threshold (<0.3%).

Bond length and angle quality were excellent in both models, with no bad bonds detected and only 0.35% (EmCOASY) and 0.43% (HsCOASY) of bond angles falling outside the ideal range—values slightly above the <0.1% target. No Cβ deviations (>0.25 Å) or cis-proline anomalies were observed in either structure, further supporting correct local stereochemistry.

CaBLAM outliers, an indicator of local backbone geometry often sensitive to low-resolution models, were slightly elevated at 1.5% for EmCOASY and 1.4% for HsCOASY (goal <1.0%). Additionally, CA geometry outliers were modestly above optimal for EmCOASY (0.57%) but acceptable for HsCOASY (0.18%) **(Table S2).**

Overall, both EmCOASY and HsCOASY structures displayed strong stereochemical quality and geometric fidelity. While minor deviations from ideal values were noted in certain parameters, particularly in backbone geometry, these were within acceptable tolerances and do not compromise the validity of the models for subsequent structure-based drug discovery workflows.

Pocket analysis

The comparative pocket analysis between *Echinococcus multilocularis* Dephospho-CoA kinase (EmCOASY) and human Dephospho-CoA kinase (HmCOASY) revealed distinct differences in binding site geometry and residue composition. The predicted binding pocket of EmCOASY (**Figure S3A**) exhibited a solvent-accessible surface area of 899.41 Å² and a volume of 1857.09 Å³, indicating a moderately open and spacious cavity. In contrast, the pocket of HmCOASY (**Figure S3B)** was characterized by a larger area of 1382.53 Å² and a significantly higher volume of 2725.84 Å³, suggesting a deeper and more extended binding groove. This structural divergence may reflect functional specialization or differential ligand adaptability between the two species.

Residue-level inspection of the pockets revealed that EmCOASY's pocket was composed of 54 residues, notably enriched in polar and hydrophobic amino acids such as MET1, CYS69, VAL205, and PHE293, which contribute to potential hydrogen bonding and hydrophobic interactions with ligands. Meanwhile, the HmCOASY pocket contained 75 residues, including prominent charged and aromatic side chains like ARG202, PHE254, and TRP536. These additional residues in HmCOASY not only expand the interaction surface but may also affect the ligand selectivity and binding energetics. Notably, overlapping conserved residues such as LYS208, ARG305, and LEU307 suggest core functional constraints across both homologs (**Figure S3)**.

Collectively, the comparative analysis highlights EmCOASY as a structurally compact but functionally viable target, while the extended pocket of HmCOASY may offer broader ligand accommodation, potentially increasing off-target risk in drug development. These insights support the

rationale for selective targeting strategies **(Table S3)**

Ligand Identification and ADMET Profiling

An initial pool of 419 phytochemical candidates with potential antimalarial activity was compiled through literature mining and the Dr. Duke's Phytochemical and Ethnobotanical database. These candidates were subsequently validated via the PubChem database, where chemical identifiers such as Compound IDs (CIDs) and SMILES strings were retrieved. This process refined the dataset to 297 structurally confirmed compounds suitable for computational modeling and docking.

Out of the 297 structurally confirmed ligands, a stepwise ADMET screening was conducted to ensure optimal pharmacokinetic and toxicity profiles for drug-likeness evaluation. In the first stage, the compounds were screened using SwissADME based on absorption-related criteria such as blood-brain barrier (BBB) permeability, gastrointestinal (GI) absorption, and Lipinski's Rule of Five. Compounds failing to meet these critical pharmacokinetic requirements were excluded, resulting in a narrowed set of 49 ligands with acceptable ADME properties. These 49 ligands were then subjected to a second-level toxicity assessment using pkCSM, focusing on safety-related endpoints including AMES mutagenicity, hepatotoxicity, and skin sensitization. Compounds that showed any positive toxicity predictions in these categories were removed from further analysis. Following this toxicity-based filtering, 19 ligands were finally retained as high-quality candidates, exhibiting both favorable pharmacokinetics and non-toxic profiles. These ligands were selected for downstream docking and simulation studies to evaluate their therapeutic potential (**Table S4).**

Molecular Docking Study and Decoy analysis

A comparative molecular docking analysis was conducted to assess the binding affinities of 19 phytochemicals against *Echinococcus multilocularis* CoA synthase (EmCoASY) and the human homolog (HsCoASY), using the best-performing decoy compound as a reference. Among these, Quercetin (CID: 5280343) demonstrated the highest binding affinity toward EmCoASY at –9.4 kcal/mol, notably surpassing the decoy's –8.4 kcal/mol, and exhibited a favorable selectivity margin over HsCoASY (–8.2 kcal/mol). Chaparrinone (CID: 73154) and (Z)-1,3-Bis(4-hydroxyphenyl)-1,4-pentadiene (CID: 6440617) also displayed strong and selective interactions with EmCoASY, with binding energies of –8.9 and –8.2 kcal/mol, respectively, while maintaining weaker affinities for HsCoASY. Artesunate (CID: 6917864), a known antimalarial, similarly showed a promising binding score (–8.2 kcal/mol for EmCoASY vs. –7.1 for HsCoASY), validating the screening approach. In contrast, compounds like Limonin, Ailanthone, and Methylandolensate bound more tightly to the human homolog, indicating lower specificity. Several other candidates, including Nimbinin, Eupatorin, and Acacetin, though exhibiting moderate affinity, failed to outperform the decoy or lacked target selectivity. Taken together, these findings highlight Quercetin, Chaparrinone, Artesunate, and (Z)-1,3-Bis(4-hydroxyphenyl)-1,4-pentadiene as potential lead candidates for further validation based on both binding strength and selectivity toward the parasitic target **(Table 1)**.

To further validate the docking outcomes, detailed interaction profiling of the top four ligands—Chaparrinone (CID: 73154), Quercetin (CID: 5280343), (Z)-1,3-Bis(4-

hydroxyphenyl)-1,4-pentadiene (CID: 6440617), and Artesunate (CID: 6917864)—was performed (**Figure 1**). These molecules demonstrated diverse and stabilizing interactions within the EmCoASY active site. Chaparrinone **(Figure 1A)** formed strong conventional hydrogen bonds with HIS188 (1.94 Å), HIS446 (2.11 Å), and SER447 (3.35 Å), in addition to a π-alkyl interaction with MET472 (4.27 Å), suggesting a stable and snug binding conformation. Quercetin (**Figure 1B)** established hydrogen bonds with ASP478 (2.25 Å), SER473 (2.66 Å), and MET472 (3.55 Å), while π–π stacking with TRP480 (4.60 Å) and a short-range interaction with LEU192 (1.59 Å) highlighted both favorable and unfavorable contacts.

(Z)-1,3-Bis(4-hydroxyphenyl)-1,4-pentadiene (**Figure 1C**) showed hydrogen bonding with ASP478 (1.99 Å) and SER473 (2.00 Å), with π-π stacking and alkyl contacts ranging from 4.37 Å to 5.31 Å. Artesunate (**Figure 1D)** displayed hydrogen bonds with GLU448 (2.23 Å), SER447 (2.49 Å), and HIS446 (2.17 Å), along with π-stacking to TRP480 (5.15 Å) and hydrophobic contacts to PRO445 and PHE443 at distances between 4.61 Å and 5.22 Å. These bond distances, particularly those under 3.5 Å, support strong ligand-residue affinity, confirming the robust and specific binding of these phytochemicals to EmCoASY (**Figure 1).**

Molecular Dynamics Simulation Studies

To evaluate the physicochemical compatibility of selected top ligands within the EmCoASY pocket, hydrophobicity surface mapping and binding orientation visualization were conducted (**Figure 2).** The EmCoASY pocket displayed a mixed surface topology comprising both hydrophobic and hydrophilic regions. Ligands such as Chaparrinone and (Z)-1,3-Bis(4-hydroxyphenyl)-1,4-pentadiene primarily aligned with the hydrophobic core, enhancing van der Waals and π-interactions. In contrast, ligands like Quercetin and Artesunate showed a preference for peripheral polar zones, anchoring through multiple hydrogen bonds. This spatial orientation suggests a strong role of charge distribution and hydrophobic matching in stabilizing ligand binding. The combination of polar functional groups and hydrophobic scaffolds enabled optimal interaction profiles, indicating a well-balanced ligand-pocket complementarity that supports the selection of these candidates for further dynamic and functional analysis (**Figure 2).**

A 200 ns molecular dynamics simulation was conducted to evaluate the structural stability and flexibility of EmCoASY in complex with the selected four ligands using RMSD and RMSF analyses.

To evaluate the conformational stability of the EmCoASY protein in complex with the four selected ligands—Chaparrinone (CID: 73154), Quercetin (CID: 5280343), (Z)-1,3-Bis(4-hydroxyphenyl)-1,4-pentadiene (CID: 6440617), and Artesunate (CID: 6917864)—root mean square deviation (RMSD) and root mean square fluctuation (RMSF) analyses were conducted across a 200 ns molecular dynamics simulation.

The RMSD profiles (**Figure 3A**) demonstrated marked differences in global stability among the ligand-bound complexes. The Chaparrinone-bound complex exhibited the lowest and most stable RMSD trajectory, fluctuating consistently between 0.6 and 1.1 nm, indicating minimal structural deviation throughout the simulation. Artesunate also maintained stability with RMSD values ranging from 1.0 to 1.5 nm, suggesting a stable binding conformation. In contrast, both Quercetin and 6440617 initially showed sharp RMSD rises, peaking near 5.5 nm and 5.1 nm, respectively, during the early phase of simulation. However, after 55 ns, both complexes stabilized, showing

RMSD plateaus around 3.8–4.0 nm, reflecting initial conformational rearrangements before reaching equilibrium.
RMSF analysis further illuminated the residue-level flexibility patterns for each complex **(Figure 3B**). Across all systems, fluctuations were modest, with most residues maintaining RMSF values between 0.1 and 0.4 nm. The highest fluctuations were observed at the N- and C-terminal regions, as expected due to their intrinsic flexibility, with values peaking around 2.0 nm. Notably, the Chaparrinone and Artesunate complexes exhibited lower RMSF values across the catalytic core, reflecting more rigid and compact interactions. In contrast, Quercetin and 6440617 showed slightly elevated fluctuations in specific loop regions, which correlated with their greater initial RMSD deviations. Collectively, these findings suggest that Chaparrinone and Artesunate formed the most conformationally stable interactions with EmCoASY, whereas Quercetin and 6440617 induced more extensive structural rearrangements but eventually settled into relatively stable binding poses.
SASA values provide an estimate of the exposure of protein residues to the solvent environment, reflecting conformational openness or burial during simulation. All four complexes maintained relatively stable SASA values throughout 200 ns, with minor fluctuations indicative of dynamic but overall preserved structures. Numerically, SASA values ranged between 288 nm² and 303 nm² for all systems. The artesunate-bound complex (CID: 6917864) exhibited the highest average SASA (~297–300 nm²), suggesting increased surface residue exposure, possibly due to enhanced loop flexibility or partial unfolding. In contrast, chaparrinone (CID: 73154) and quercetin (CID: 5280343) complexes exhibited slightly lower average SASA values, clustered around 293–295 nm², indicating a relatively more compact and less solvent-exposed core. The (Z)-1,3-Bis(4-hydroxyphenyl)-1,4-pentadiene complex (CID: 6440617) displayed intermediate SASA values within the same overall range (**Figure 4A).**
The Rg parameter measures the overall compactness of the protein-ligand complex. During the 200 ns simulation, Rg values for all complexes ranged from 2.77 nm to 2.95 nm. Artesunate (CID: 6917864) yielded the lowest and most stable Rg, averaging approximately 2.84 nm, suggesting a highly compact and structurally rigid complex. Both quercetin (CID: 5280343) and chaparrinone (CID: 73154) maintained similarly stable Rg values, centered around 2.85–2.87 nm, indicating good structural integrity and compactness. Conversely, the complex with (Z)-1,3-Bis(4-hydroxyphenyl)-1,4-pentadiene (CID: 6440617) had the highest mean Rg value (about 2.93 nm), reflecting increased conformational flexibility and slight tendencies toward minor unfolding or expansion during the simulation (**Figure 4B).**
Hydrogen bonds are critical determinants of protein–ligand binding affinity and stability. The number of hydrogen bonds formed between the protein and each ligand was monitored throughout the simulation. The quercetin complex (CID: 5280343) demonstrated the highest and most persistent hydrogen bonding, consistently forming 3 to 7 bonds, indicative of robust and stable interactions. Chaparrinone (CID: 73154) maintained a favorable profile as well, with 2 to 4 hydrogen bonds present for most of the trajectory. In contrast, artesunate (CID: 6917864) and (Z)-1,3-Bis(4-hydroxyphenyl)-1,4-pentadiene (CID: 6440617) exhibited fewer and less stable hydrogen bonds, typically fluctuating between 1 and 3, with more frequent

intervals of reduced bonding. These results suggest that quercetin exhibits superior hydrogen bonding capacity, potentially underpinning its greater overall binding stability compared to the other ligands **(Figure 4C).**

Taken together, the SASA, Rg, and hydrogen bond analyses illustrate that quercetin and chaparrinone foster more compact and stable complexes with the protein, as evidenced by their moderate SASA and Rg values and persistent hydrogen bonding. Artesunate, while highly compact, demonstrates increased solvent exposure and less stable hydrogen bonding. The (Z)-1,3-Bis(4-hydroxyphenyl)-1,4-pentadiene complex, although flexible, displays the least compactness and weaker bonding profile. These findings provide quantitative support for the relative stability and interaction quality of each protein–ligand complex **(Figure 4)**

Principal Component and Covariance Analysis

Covariance analysis provides a deeper understanding of correlated motions between residues during molecular dynamic (MD) simulations. By evaluating the covariance of atomic displacements, the method identifies the extent to which movements of residues are interdependent—either positively (moving together) or negatively (moving oppositely). This approach is particularly useful for revealing functionally relevant flexibility and domain motions in protein-ligand complexes.

In the present study, the covariance matrices for EmCoASY in complex with chaparrinone and artesunate are depicted. The color gradients represent the strength and direction of the correlated atomic displacements, where red regions indicate positive correlations and blue regions indicate anti-correlated motions.

The chaparrinone-bound complex (**Figure 5A)** showed a balanced mixture of correlated and anti-correlated motions, suggesting organized and cooperative internal dynamics, with relatively strong coordinated motion across certain residue blocks. This reinforces the stability observed in the RMSD and Rg analyses.

In contrast, the artesunate complex (**Figure 5B)** displayed more dispersed and less intense correlations, implying moderate internal flexibility and reduced cooperativity in residue motion. Despite this, artesunate maintained acceptable dynamic behavior throughout the simulation.

Overall, the covariance matrices support the conclusion that chaparrinone exhibits more coherent internal dynamics within EmCoASY, aligning with its favorable performance in PCA and hydrogen bonding analyses.

Principal Component Analysis (PCA) is a dimensionality-reduction technique frequently employed in molecular dynamics (MD) to extract major patterns of atomic motion from large trajectory datasets. By projecting trajectories along eigenvectors (principal components), PCA identifies dominant collective fluctuations in the protein-ligand system, offering insights into structural flexibility and motion trends during simulation. The PCA projection of protein-ligand complexes bound to *chaparrinone* and *artesunate* is shown in **Figure 5C-D.** For the *chaparrinone*-bound complex**,** the first three principal components (PC1, PC2, and PC3) captured 27.9%, 10.78%, and 9.42% of the total variance, respectively. The scatter plots showed a relatively compact and symmetrical cluster with smooth transitions between conformational states, indicating limited structural drift and stable binding behavior over the 200 ns MD simulation **(Figure 5C).**

In comparison, the *artesunate* complex (**Figure 5D)** exhibited principal variances of 22.19%, 14.99%, and 12.2% for PC1, PC2, and PC3, respectively. The conformational space sampled by *artesunate* was slightly broader but still well-distributed, signifying moderate flexibility within a stable binding region. The scree plots in both cases suggest that the dominant motions are largely contained within the first few PCs, supporting convergence and controlled structural deviations (**Figure 5**).

Together, the PCA outcomes support the stability of both chaparrinone and artesunate interactions with EmCoASY, with the former showing slightly more compact conformational behavior, aligning with RMSD and Rg results.

MMGBSA Analysis

The MM/GBSA energy decomposition analysis for the EmCoASY–ligand complexes with chaparrinone and artesunate demonstrated distinct thermodynamic binding profiles. The calculated binding free energy (ΔG_bind) for chaparrinone was -71.68 kcal/mol, indicating a strong and energetically favorable interaction within the binding pocket. In comparison, artesunate yielded a ΔG_bind of -66.42 kcal/mol, suggesting moderately stable complex formation. The van der Waals contribution was more pronounced in chaparrinone (-7.89 kcal/mol) relative to artesunate (-6.94 kcal/mol), reflecting tighter nonpolar interactions in the former.

Electrostatic interactions slightly favored artesunate, contributing -6.02 kcal/mol versus -5.27 kcal/mol for chaparrinone, indicating enhanced polar contact for artesunate. However, hydrophobic interactions dominated the binding energetics in both cases, contributing -36.71 kcal/mol and -31.88 kcal/mol for chaparrinone and artesunate, a stronger affinity of chaparrinone for the hydrophobic regions of the pocket. The solvation energy penalties (ΔG_solv) were comparable at 24.19 kcal/mol for chaparrinone and 23.40 kcal/mol for artesunate, suggesting similar levels of desolvation cost upon binding.

Overall, chaparrinone demonstrated a more energetically favorable interaction with EmCoASY, with a ΔΔG_bind of -5.26 kcal/mol when compared to artesunate, largely attributed to its superior van der Waals and lipophilic stabilization effects **(Table 2)**.

Table 1: Docking analysis along with the Decoy affinity for selected compound.

Chemical	CID	EmCoASY Binding (kcal/mol)	HsCoASY Binding (kcal/mol)	Decoy Best Affinity (kcal/mol)	Selected
Chaparrinone	73154	**-8.9**	-8.5	-7.9	Potent candidate
Quercetin	5280343	**-9.4**	-8.2	-8.4	Potent candidate
Limonin	179651	-8.3	**-9.2**	-8.8	(HsCoASY > EmCoASY)
Ailanthone	72965	-8.2	**-9.1**	-8.7	(HsCoASY > EmCoASY)
(Z)-1,3-Bis(4-Hydroxyphenyl)-1,4-Pentadiene	6440617	**-8.2**	-6.9	-7.2	Potent candidate
Artesunate	6917864	**-8.2**	-7.1	-6.7	Potent candidate
Nimbinin	49863985	-8.0	-8.6	-9.0	Worse than

Chemical	CID	EmCoASY Binding (kcal/mol)	HsCoASY Binding (kcal/mol)	Decoy Best Affinity (kcal/mol)	Selected
					decoy
Eupatorin	97214	-7.9	-7.7	-8.9	Worse than decoy
Acacetin	5280442	-7.9	-7.9	-8.9	Worse than decoy
Cirsilineol	162464	-7.7	-7.9	-6.7	HsCoASY > EmCoASY
Chrysosplenetin	5281608	-7.7	-7.9	-6.7	HsCoASY > EmCoASY)
Methylangolensate	21596327	-7.7	-9.0	-6.7	HsCoASY > EmCoASY)
Casticin	5315263	-7.6	-8.0	-6.4	HsCoASY > EmCoASY)
Nimbandiol	157277	-7.5	-7.8	-6.3	HsCoASY > EmCoASY)
Neurolenin-A	71306326	-7.1	-7.6	-5.9	HsCoASY > EmCoASY)
Ajugarin-I	173866	-6.9	-8.1	-6.8	HsCoASY > EmCoASY)
Nimocinol	178770	-6.9	-7.4	-6.8	HsCoASY > EmCoASY)
Neurolenin-B	49799795	-6.8	-7.2	-6.7	HsCoASY > EmCoASY)
Colchicine	6167	-6.5	-7.3	-6.4	HsCoASY > EmCoASY)

Table 2: MMGBSA Analysis of Chaparrinone and Artesunate.

Energy Component	Chaparrinone (kcal/mol)	Artesunate (kcal/mol)
Binding Free Energy (ΔG_bind)	-71.68	-66.42
Van der Waals (vdW)	-7.89	-6.94
Electrostatic (Coulomb)	-5.27	-6.02
Hydrophobic (Lipo)	-36.71	-31.88
Solvation Free Energy (ΔG_solv)	24.19	23.40
ΔΔG_bind (ΔG_chaparrinone - ΔG_artesunate)	-5.26	—

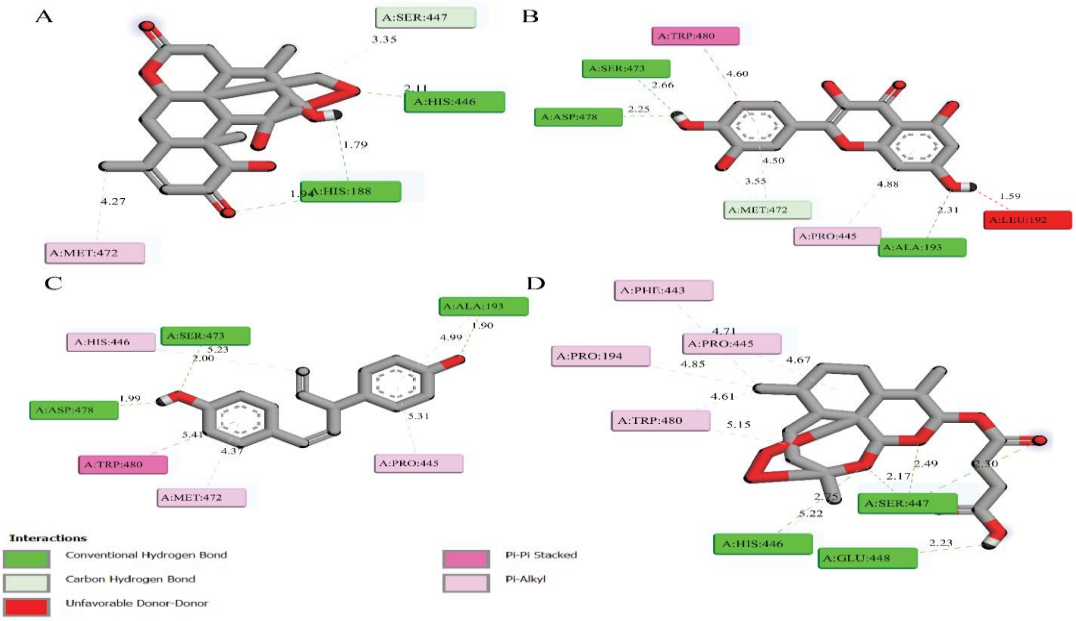

Figure 1. 2D interaction profile of top ligand with EmCoASY. (A) Chaparrinone (CID: 73154), (B) Quercetin (CID: 5280343), (C) (Z)-1,3-Bis(4-hydroxyphenyl)-1,4-pentadiene (CID: 6440617), and (D) Artesunate (CID: 6917864). Key interactions include conventional hydrogen bonds (green), carbon hydrogen bonds (light blue), π-π stacking (magenta), and π-alkyl or alkyl interactions (violet). Unfavorable donor-donor contacts are shown in red. Distances (in Å) between ligand atoms and protein residues are labeled, indicating the strength and proximity of binding interactions.

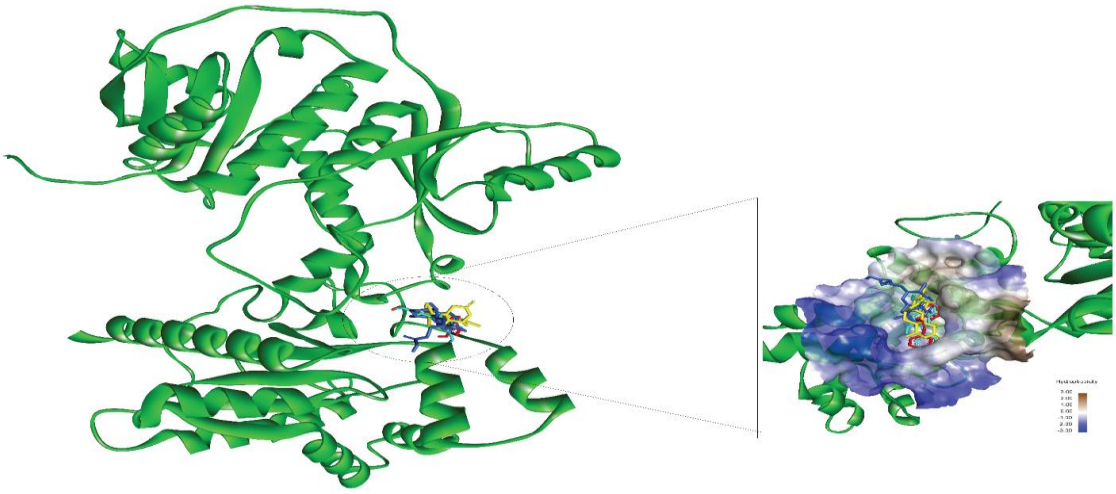

Figure 2. Hydrophobicity surface analysis and docking orientation of selected top ligands within the EmCoASY binding pocket. The protein is represented in green cartoon form with the binding site highlighted. The inset shows a close-up surface view of the binding cavity colored according to hydrophobic potential (blue: hydrophilic; white: neutral; brown: hydrophobic). The four top-performing ligands are overlaid to visualize docking orientation and chemical compatibility within the hydrophobic microenvironment: yellow – Chaparrinone (CID: 73154), cyan – Quercetin (CID: 5280343), red – (Z)-1,3-Bis(4-hydroxyphenyl)-1,4-pentadiene (CID: 6440617), and blue – Artesunate (CID: 6917864). This comparative visualization highlights the alignment and interaction tendencies of each ligand relative to the hydrophobic and polar regions of the target binding pocket.

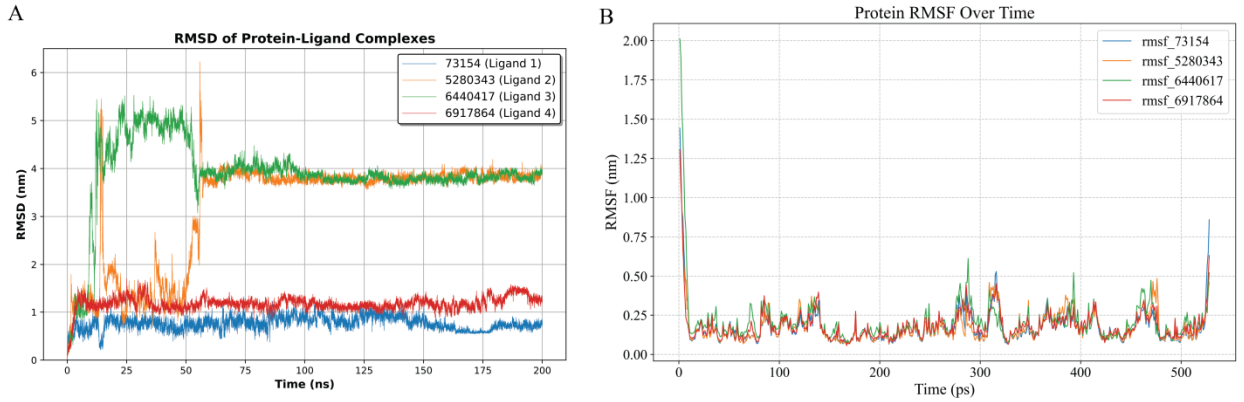

Figure 3. A 200 ns molecular dynamics simulation selected four ligands RMSD and RMSF analyses. (A) RMSD plot showing the structural stability of emcoasy in complex with chaparrinone (73154, blue), quercetin (5280343, orange), (z)-1,3-bis(4-hydroxyphenyl)-1,4-pentadiene (6440617, green), and artesunate (6917864, red) over a 200 ns simulation. (B) RMSF plot illustrating residue-wise flexibility for the same four ligand-bound complexes.

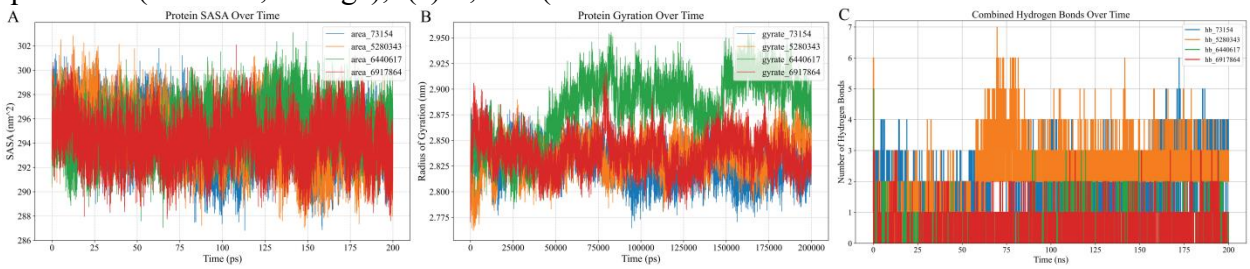

Figure 4. Structural and interaction analysis of four protein–ligand complexes over 200 ns molecular dynamics simulation. (A) Solvent-accessible surface area (SASA) trajectories, showing the dynamic exposure of protein surface residues to solvent. (B) Radius of gyration (Rg) profiles, reflecting the overall compactness and structural stability of each complex during the simulation. (C) Time evolution of the number of hydrogen bonds between protein and ligand, highlighting the stability and persistence of binding interactions. Ligands analyzed include chaparrinone (CID: 73154), quercetin (CID: 5280343), (Z)-1,3-Bis(4-hydroxyphenyl)-1,4-pentadiene (CID: 6440617), and artesunate (CID: 6917864).

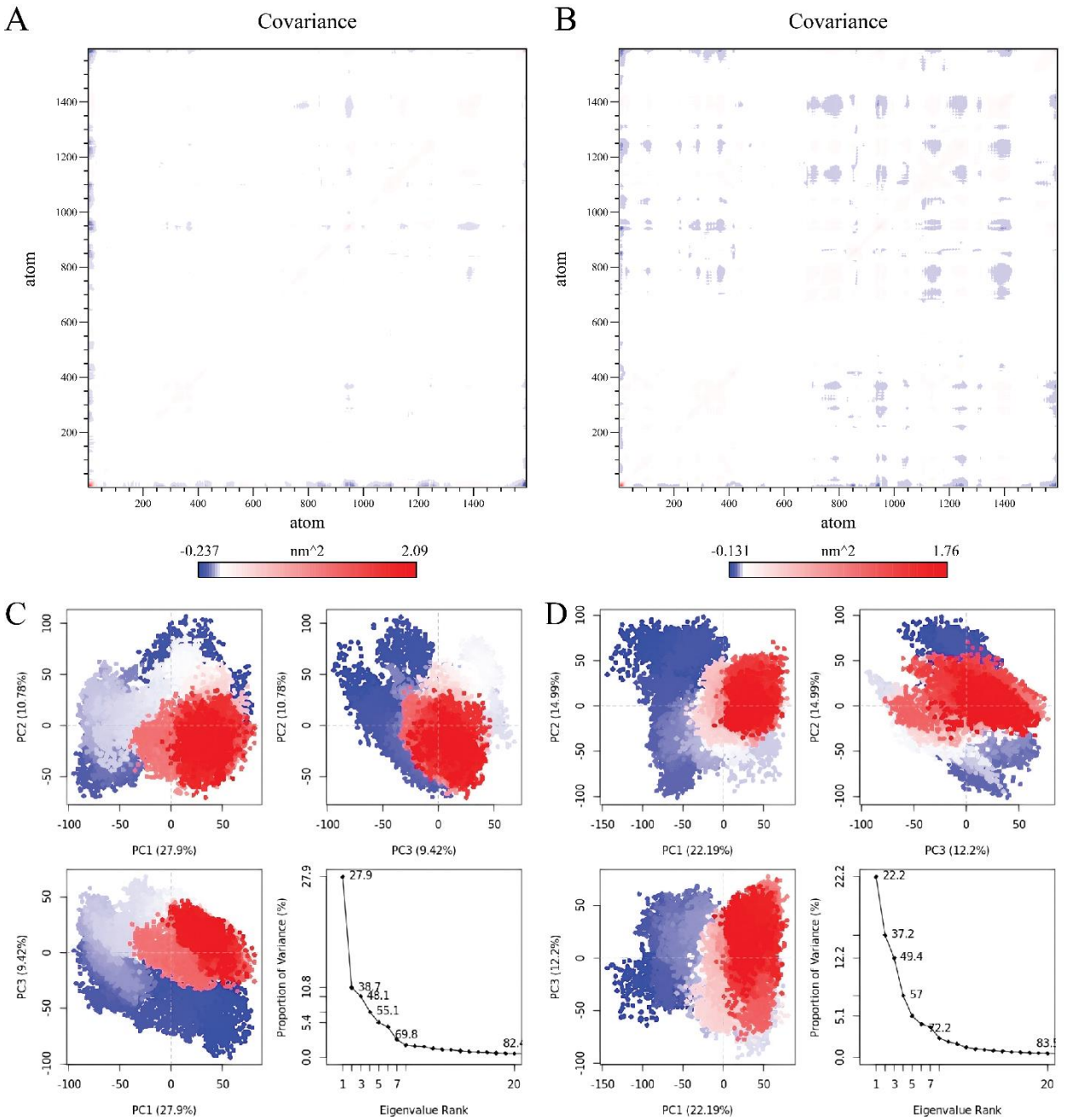

Figure 5. Principal component and covariance analyses of EmCoASY-ligand complexes during 200 ns MD simulations. (A) chaparrinone (CID: 73154); **(B)** artesunate (CID: 6917864).

Each matrix visualizes pairwise residue motion correlation during the 200 ns MD simulation. Red regions represent positively correlated atomic movements, blue indicates anti-correlated motions, and white regions show little to no correlation. The analysis highlights differences in global dynamic behavior between the two complexes. **(C)** chaparrinone (CID: 73154): PCA scatter plots of PC1 vs PC2, PC1 vs PC3, and PC2 vs PC3 along with the corresponding eigenvalue (scree) plot. **(D)** artesunate (CID: 6917864): same PCA projections and variance plots. Color gradients represent temporal transitions across the MD trajectory, from blue (initial frames) to red (later frames). The scree plots highlight that the majority of the structural variance is concentrated within the top three components.

DISCUSSION

Alveolar echinococcosis, caused by *Echinococcus multilocularis*, is a life-threatening zoonotic disease with limited treatment options, often relying on benzimidazole-based therapy and surgical intervention. These strategies are associated with significant limitations, such as toxicity, poor patient tolerance, and parasite recurrence[38,39]. The rising concern of drug resistance underscores the urgent need for novel, selective therapeutic agents that target parasite-specific proteins without affecting human homologs. In this study, we employed a robust in silico pipeline to identify potential inhibitors targeting *E. multilocularis* Dephospho-CoA kinase (EmCoASY), a parasite-specific enzyme involved in the CoA biosynthesis pathway and mitochondrial metabolism[40–42].

Our computational approach leveraged comparative genomics and protein domain analysis to identify EmCoASY as a promising drug target due to its essentiality and structural divergence from the human ortholog (HsCoASY). Homology modeling using AlphaFold provided a high-confidence 3D structure, with druggable pockets predicted using CASTp. A large phytochemical ligand library was curated through literature and public repositories, followed by ADMET screening. Out of an initial set of 297 candidates, 20 ligands passed stringent pharmacokinetic and toxicity filters. This refined subset was subjected to molecular docking against both EmCoASY and HsCoASY to ensure target selectivity.

Among the screened compounds, four ligands—chaparrinone (CID: 73154), quercetin (CID: 5280343), (Z)-1,3-bis(4-hydroxyphenyl)-1,4-pentadiene (CID: 6440617), and artesunate (CID: 6917864)—showed strong binding affinities with EmCoASY, with binding energies ranging from -8.2 to -9.4 kcal/mol. Notably, chaparrinone and artesunate demonstrated selectivity by exhibiting higher affinity for EmCoASY compared to HsCoASY and also surpassed the best binding affinity of decoy ligands, suggesting their potential as selective inhibitors. Structural visualization and hydrogen bond analysis confirmed stable binding interactions in the ATP-binding cleft of the parasite enzyme.

Molecular dynamics (MD) simulations over 200 ns revealed stable root mean square deviation (RMSD) values for the protein–ligand complexes, especially those involving chaparrinone and artesunate, indicating stable binding conformations. Root means square fluctuation (RMSF) and radius of gyration (Rg) analyses further supported the conformational stability and compactness of the protein-ligand complexes. Hydrophobic surface analysis revealed key non-polar residues lining the binding pocket, which likely enhanced van der Waals and lipophilic interactions. Electrostatic surface mapping demonstrated favorable charge complementarity between the ligands and the pocket residues.

The principal component analysis (PCA) showed that protein motions in ligand-bound states were more confined compared to the apo form, reflecting reduced conformational freedom due to ligand binding. Covariance and dynamic cross-correlation analysis (DCCM) illustrated dampened long-range motions in the chaparrinone and artesunate complexes, implying a stabilizing effect. MM-GBSA calculations revealed binding free energies of –kcal/mol for chaparrinone and -71.1 kcal/mol for artesunate, with strong hydrophobic and van der Waals contributions dominating the interaction energetics. These findings reinforce the superior binding profile and stability of these ligands.

This study provides a comprehensive computational framework for anti-echinococcal drug discovery, targeting a

non-human essential kinase. The selected compounds exhibit favorable drug-like properties, stable binding, and strong energetics, making them promising candidates for further optimization. Importantly, the selective targeting of parasite kinases may reduce the likelihood of host toxicity, addressing a major limitation of current therapies[43–45].

A comprehensive survival analysis conducted in Switzerland over a 50-year period revealed that while benzimidazole therapy has significantly improved the prognosis of AE patients, early curative surgery did not confer a survival benefit specific to AE. The study also noted an increase in incidental diagnoses, suggesting improved imaging techniques and awareness[46] . A 2023 case report from Italy documented an autochthonous human AE case in a patient with no history of travel abroad, indicating the parasite's spread to previously non-endemic areas[4]. This underscores the importance of heightened surveillance and diagnostic vigilance even in regions traditionally considered free from AE. Recent research has identified threonine dehydrogenase (EmTDH) as a potential drug target in *E. multilocularis*. The study demonstrated that the parasite's metacestode stage relies heavily on threonine metabolism, and inhibiting EmTDH could impair parasite viability. This opens avenues for targeted drug development against AE. Despite the efficacy of benzimidazole compounds like albendazole and mebendazole, their parasitostatic nature necessitates prolonged treatment durations, often leading to patient non-compliance and potential relapse[39,47].

However, this study is not without limitations. The predictions are entirely in silico, and experimental validation is required to confirm in vivo efficacy and pharmacodynamics. Additionally, although our target shows low homology with human proteins, off-target effects cannot be completely ruled out. Future studies should involve biochemical assays, cytotoxicity tests, and structure-activity relationship (SAR) modeling to refine these compounds further.

CONCLUSIONS

This study employed an integrative computational approach to identify and characterize potential phytochemical inhibitors targeting *Echinococcus multilocularis* CoA synthase (EmCoASY), a key enzyme implicated in the pathogenesis of alveolar echinococcosis. Through a comprehensive virtual screening of 419 natural compounds, 20 candidates were shortlisted based on favorable ADMET profiles and docking affinities. Among them, chaparrinone and artesunate exhibited the most promising binding energies against EmCoASY, outperforming standard decoys and demonstrating selectivity over human homolog. Given the limitations of current AE treatments, such as the parasitostatic effect and hepatotoxicity of benzimidazoles, these findings open new avenues for phytochemical-based drug development.

Conflict of Interest: The author declares no conflict of interest.

Financial Disclosure: The author received no specific funding for this work.

Ethics Approval:

Consent for Publication: Not applicable.

Data Availability: All the data will be available without any restrictions.

REFERENCES

1. Rostami A, Lundström-Stadelmann B, Frey CF, Beldi G, Lachenmayer A, Chang BCH, et al. Human Alveolar Echinococcosis—A Neglected Zoonotic Disease Requiring Urgent Attention. Int J Mol Sci. 2025 Mar 19;26(6):2784.

2. Torgerson PR, Schweiger A, Deplazes P, Pohar M, Reichen J, Ammann RW, et al. Alveolar echinococcosis: From a deadly disease to a well-controlled infection. Relative survival and economic analysis in Switzerland over the last 35 years. J Hepatol. 2008 Jul 1;49(1):72–7.

3. Eckert J, Deplazes P. Biological, Epidemiological, and Clinical Aspects of Echinococcosis, a Zoonosis of Increasing Concern. Clin Microbiol Rev. 2004 Jan;17(1):107–35.
4. Tamarozzi F, Ronzoni N, Degani M, Oliboni E, Tappe D, Gruener B, et al. Confirmed Autochthonous Case of Human Alveolar Echinococcosis, Italy, 2023. Emerg Infect Dis. 2024 Feb;30(2):350–3.
5. Wen H, Vuitton L, Tuxun T, Li J, Vuitton DA, Zhang W, et al. Echinococcosis: Advances in the 21st Century. Clin Microbiol Rev. 2019 Feb 13;32(2):10.1128/cmr.00075-18.
6. Nurkanto A, Imamura R, Rahmawati Y, Prabandari EE, Waluyo D, Annoura T, et al. Dephospho-Coenzyme A Kinase Is an Exploitable Drug Target against: Identification of Selective Inhibitors by High-Throughput Screening of a Large Chemical Compound Library. Antimicrob Agents Chemother. 2022 Nov 15;66(11):e0042022.
7. Bostancioglu SM, Mutlu O. Exploring novel inhibitors for lactate dehydrogenase: a computational structural biology perspective. Parasitol Res. 2025 Jan 7;124(1):1.
8. Chaudhry S, Zurbriggen R, Preza M, Kämpfer T, Kaethner M, Memedovski R, et al. Dual inhibition of the energy metabolism. Front Vet Sci [Internet]. 2022 Aug 5 [cited 2025 Jun 4];9. Available from: https://www.frontiersin.org/journals/veterinary-science/articles/10.3389/fvets.2022.981664/full
9. Vuitton DA, Gottstein B. and Its Intermediate Host: A Model of Parasite-Host Interplay. J Biomed Biotechnol. 2010;2010:923193.
10. Borkakoti N, Thornton JM. AlphaFold2 protein structure prediction: Implications for drug discovery. Curr Opin Struct Biol. 2023 Feb 1;78:102526.
11. van Breugel M, Rosa e Silva I, Andreeva A. Structural validation and assessment of AlphaFold2 predictions for centrosomal and centriolar proteins and their complexes. Commun Biol. 2022 Apr 5;5:312.
12. Torres PHM, Sodero ACR, Jofily P, Silva-Jr FP. Key Topics in Molecular Docking for Drug Design. Int J Mol Sci. 2019 Sep 15;20(18):4574.
13. Rao SN, Head MS, Kulkarni A, LaLonde JM. Validation Studies of the Site-Directed Docking Program LibDock. J Chem Inf Model. 2007 Nov 1;47(6):2159–71.
14. de Vries LE, Lunghi M, Krishnan A, Kooij TWA, Soldati-Favre D. Pantothenate and CoA biosynthesis in Apicomplexa and their promise as antiparasitic drug targets. PLoS Pathog. 2021 Dec 30;17(12):e1010124.
15. Xiao SH, Feng JJ, Guo HF, Jiao PY, Yao MY, Jiao W. Effects of mebendazole, albendazole, and praziquantel on succinate dehydrogenase, fumarate reductase, and malate dehydrogenase in cysts harbored in mice. Zhongguo Yao Li Xue Bao. 1993 Mar 1;14(2):151–4.
16. Wani JH, Srivastava VM. Effect of cations and anthelmintics on enzymes of respiratory chains of the cestode. Biochem Mol Biol Int. 1994 Sep 1;34(2):239–50.
17. Harris TW, Lee R, Schwarz E, Bradnam K, Lawson D, Chen W, et al. WormBase: a cross-species database for comparative genomics. Nucleic Acids Res. 2003 Jan 1;31(1):133–7.
18. Harris TW, Arnaboldi V, Cain S, Chan J, Chen WJ, Cho J, et al. WormBase: a modern Model Organism Information Resource. Nucleic Acids Res. 2020 Jan 8;48(D1):D762–7.
19. Harris TW, Chen N, Cunningham F, Tello-Ruiz M, Antoshechkin I, Bastiani C, et al. WormBase: a multi-species resource for nematode biology and genomics. Nucleic Acids Res. 2004 Jan 1;32(Database issue):D411-417.
20. Skolnick J, Gao M, Zhou H, Singh S. AlphaFold 2: Why It Works and Its Implications for Understanding the Relationships of Protein Sequence, Structure, and Function. J Chem Inf Model. 2021 Oct 25;61(10):4827–31.
21. Yang Z, Zeng X, Zhao Y, Chen R. AlphaFold2 and its applications in the fields of biology and medicine. Signal Transduct Target Ther. 2023 Mar 14;8(1):1–14.
22. Jumper J, Evans R, Pritzel A, Green T, Figurnov M, Ronneberger O, et al. Highly accurate protein structure prediction with AlphaFold. Nature. 2021 Aug;596(7873):583–9.
23. Sievers F, Wilm A, Dineen D, Gibson TJ, Karplus K, Li W, et al. Fast, scalable generation of high-quality protein multiple sequence alignments using Clustal Omega. Mol Syst Biol. 2011 Oct 11;7:539.
24. Sievers F, Higgins DG. Clustal Omega for making accurate alignments of many protein sequences. Protein Sci Publ Protein Soc. 2018 Jan;27(1):135–45.
25. Davis IW, Leaver-Fay A, Chen VB, Block JN, Kapral GJ, Wang X, et al. MolProbity: all-atom contacts and structure validation for proteins and nucleic acids. Nucleic Acids Res. 2007 Jul;35(Web Server issue):W375-383.
26. Williams CJ, Headd JJ, Moriarty NW, Prisant MG, Videau LL, Deis LN, et al. MolProbity: More and better reference data for improved all-atom structure validation. Protein Sci Publ Protein Soc. 2018 Jan;27(1):293–315.
27. Ye B, Tian W, Wang B, Liang J. CASTpFold: Computed Atlas of Surface Topography

of the universe of protein Folds. Nucleic Acids Res. 2024 Jul 5;52(W1):W194–9.
28. Wiśniowska B, Linke S, Polak S, Bielecka Z, Luch A, Pirow R. Data on ADME parameters of bisphenol A and its metabolites for use in physiologically based pharmacokinetic modelling. Data Brief. 2023 Jun 1;48:109101.
29. Lucas AJ, Sproston ,Joanne L., Barton ,Patrick, and Riley RJ. Estimating human ADME properties, pharmacokinetic parameters and likely clinical dose in drug discovery. Expert Opin Drug Discov. 2019 Dec 2;14(12):1313–27.
30. Daina A, Michielin O, Zoete V. SwissADME: a free web tool to evaluate pharmacokinetics, drug-likeness and medicinal chemistry friendliness of small molecules. Sci Rep. 2017 Mar 3;7(1):42717.
31. Pires DEV, Blundell TL, Ascher DB. pkCSM: Predicting Small-Molecule Pharmacokinetic and Toxicity Properties Using Graph-Based Signatures. J Med Chem. 2015 May 14;58(9):4066–72.
32. Ekins S, Waller CL, Swaan PW, Cruciani G, Wrighton SA, Wikel JH. Progress in predicting human ADME parameters in silico. J Pharmacol Toxicol Methods. 2000 Jul 1;44(1):251–72.
33. Dallakyan S, Olson AJ. Small-Molecule Library Screening by Docking with PyRx. In: Hempel JE, Williams CH, Hong CC, editors. Chemical Biology: Methods and Protocols [Internet]. New York, NY: Springer; 2015 [cited 2025 May 31]. p. 243–50. Available from: https://doi.org/10.1007/978-1-4939-2269-7_19
34. Mysinger MM, Carchia M, Irwin JohnJ, Shoichet BK. Directory of Useful Decoys, Enhanced (DUD-E): Better Ligands and Decoys for Better Benchmarking. J Med Chem. 2012 Jul 26;55(14):6582–94.
35. Huang J, MacKerell AD. CHARMM36 all-atom additive protein force field: validation based on comparison to NMR data. J Comput Chem. 2013 Sep 30;34(25):2135–45.
36. Vanommeslaeghe K, Hatcher E, Acharya C, Kundu S, Zhong S, Shim J, et al. CHARMM General Force Field (CGenFF): A force field for drug-like molecules compatible with the CHARMM all-atom additive biological force fields. J Comput Chem. 2010 Mar;31(4):671–90.
37. Vanommeslaeghe K, MacKerell ADJr. Automation of the CHARMM General Force Field (CGenFF) I: Bond Perception and Atom Typing. J Chem Inf Model. 2012 Dec 21;52(12):3144–54.
38. Balen Topić M, Papić N, Višković K, Sviben M, Filipec Kanižaj T, Jadrijević S, et al. Emergence of in Central Continental Croatia: A Human Case Series and Update on Prevalence in Foxes. Life. 2023 Jun;13(6):1402.
39. Memedovski R, Preza M, Müller J, Kämpfer T, Rufener R, de Souza MVN, et al. Investigation of the mechanism of action of mefloquine and derivatives against the parasite *Echinococcus multilocularis*. Int J Parasitol Drugs Drug Resist. 2023 Apr 1;21:114–24.
40. Authority (EFSA) EFS, Rusinà A, Zancanaro G. Annual assessment of surveillance reports submitted in 2023 in the context of commission delegated regulation (EU) 2018/772. EFSA J. 2023;21(8):e08204.
41. Antolová D, Šnábel V, Jarošová J, Cavallero S, D'Amelio S, Syrota Y, et al. Human alveolar echinococcosis in Slovakia: Epidemiology and genetic diversity of, 2000–2023. PLoS Negl Trop Dis. 2024 Jan 10;18(1):e0011876.
42. Jing QD, A JD, Liu LX, Fan HN. Current status of drug therapy for alveolar echinococcosis. World J Hepatol. 2024 Nov 27;16(11):1243–54.
43. Ja'afaru SC, Uzairu A, Bayil I, Sallau MS, Ndukwe GI, Ibrahim MT, et al. Unveiling potent inhibitors for schistosomiasis through ligand-based drug design, molecular docking, molecular dynamics simulations and pharmacokinetics predictions. PLOS ONE. 2024 Jun 26;19(6):e0302390.
44. Chauhan V, Farooq U, Fahmi M, A K, Tripathi PK. Unveiling the anti-echinococcal efficacy of amide-based compounds: An in-silico and in-vitro study. Heliyon. 2024 May 14;10(10):e31205.
45. Zorn KM, Sun S, McConnon CL, Ma K, Chen EK, Foil DH, et al. A Machine Learning Strategy for Drug Discovery Identifies Anti-Schistosomal Small Molecules. ACS Infect Dis. 2021 Feb 12;7(2):406–20.
46. Plum PE, Ausselet N, Kidd F, Noirhomme S, Garrino MG, Dili A, et al. EchiNam: multicenter retrospective study on the experience, challenges, and pitfalls in the diagnosis and treatment of alveolar echinococcosis in Belgium. Eur J Clin Microbiol Infect Dis. 2025 Feb 1;44(2):263–75.
47. Torgerson PR, Keller K, Magnotta M, Ragland N. The Global Burden of Alveolar Echinococcosis. PLoS Negl Trop Dis. 2010 Jun 22;4(6):e722.

Citation

Mohammad M Kabli, A. Structure-Based Identification of Selective Phytochemical Inhibitors Targeting EmCoASY: A Novel Therapeutic Strategy Against Alveolar Echinococcosis. Zagazig University Medical Journal, 2025; (4420-4440): -. doi: 10.21608/zumj.2025.392468.3991